

## Monolayer surface structure analysis

G.A. Somorjai and U. Starke

Department of Chemistry and Materials Sciences Division, Lawrence Berkeley Laboratory, University of California, Berkeley, CA 94720, USA.

**Abstract.** - Modern surface science techniques provide atomic spatial resolution (scanning tunneling microscopy), improved time and energy resolution (laser spectroscopies) and determination of structure on both sides of the surface chemical bonds (tensor LEED). Solid-solid, solid-liquid, and liquid-gas interfaces are increasingly investigated in addition to the solid-gas interface. The restructuring of surfaces during chemisorption and catalytic reactions lead to the development of new dynamic models for explaining surface reactivity. The knowledge of surface structure, bonding and gas-surface interactions has been utilized to gain a better understanding of adsorption, heterogeneous catalysis, adhesion, lubrication, optical and electron transport properties. Examples will be given and discussed.

### INTRODUCTION

The structures of monolayers of atoms and molecules that are at the boundaries of solids or liquids are of great scientific and technological interest. It was Langmuir who realized around 1915 that the formation of a chemisorbed atomic layer at the surface of the tungsten filament of a lightbulb controls the dissipation of its heat<sup>1</sup>. The observation that dinitrogen had a low sticking probability on the nitrided tungsten surface led to the development of gas filled lightbulbs. His studies of chemisorption at the solid vacuum interface were well-complimented by his later investigations of the behavior of organic monolayers on water using the Langmuir trough that permits increase of the surface pressure by laterally squeezing the monolayer<sup>2</sup>. A monolayer of stearic acid spread over a lake can greatly reduce the water loss by evaporation by forming a diffusion barrier<sup>3</sup>. In addition to the solid-vacuum, solid-gas and liquid-liquid interfaces mentioned so far the structure at solid-solid interfaces controls the properties of quantum well and other microelectronic devices, adhesion and tribological properties of materials including friction, slide and lubrication. Finally solid-liquid interface structures are of great importance in electrochemistry and biology, just to mention two important fields where this type of interface predominates.

What is it that we would like to know about the atoms at these interfaces? We would like to determine their distances from their nearest neighbors on the surface and in the bulk, under the surface; their number of nearest neighbors, the nature (directionality, charge distribution, strength) of the chemical bonds that holds them in their atomic location on the surface. The atomic positions at the interface determine the electronic structure there because when the atoms move the electrons are sure to follow. We need to know what the atoms are made of, to obtain the interface composition which reveals their concentration and the presence of impurities. Ideally we would like to determine the structure and composition of each interface atom or molecule with atomic spatial resolution. Since the interface often exhibits dynamic behavior we should be able to obtain structure and composition information in a time resolved mode with atomic spatial resolution.

This goal has not been reached in surface and interface analysis as yet. However, many technology applications aiming to improve mechanical, chemical, electronic, optical and magnetic interface properties are providing incentives thereby pushing surface science in these directions.

The purpose of this paper is to review the techniques of monolayer analysis that provided most of the atomic level information so far; what is known about the surface monolayer structure and point out the future directions this field of research is likely to take.

## TECHNIQUES OF MONOLAYER ANALYSIS

Table 1 lists most of the modern surface science techniques that are utilized for monolayer analysis. The name, the abbreviation used to refer to it, a brief description of its principle of operation and the dominant information that can be obtained are all given in the Table. Electron and ion scattering techniques usually require low pressures during their application. Because of their large scattering cross sections ( $\sim 1\text{\AA}^2$ ) as compared to photons ( $\sim 10^{-6}\text{\AA}^2$ ) they are best utilized in studies of solid vacuum and solid gas interfaces. Scanning tunneling microscopy (STM) and related techniques and diffuse low energy electron diffraction (LEED) are perhaps the most rapidly developing techniques at present. STM is capable of direct imaging in real space with atomic resolution and can be employed to study solid-liquid interfaces as well.

Optical techniques are also useful for analysis of solid-liquid, solid-solid and liquid-liquid interfaces. High intensity photon beams are provided by lasers and synchrotrons and are at the frontiers of interface analysis development. Non-linear laser optics provide time resolved spectral information of interface species. Solid state NMR is particularly useful for studies of surfaces of high surface area microporous materials because usually a  $1\text{m}^2$  area is needed to obtain detectable signals due to surface species. Nevertheless this technique is becoming one of the most useful tools for studies of catalysts.

Let us now review what has been learned from the application of many of these techniques about the structure of monolayers at interfaces. Most of our information about the atomic structure comes from LEED surface crystallography studies<sup>4</sup> which have been complimented most recently by studies of the same systems using STM.

## ATOMIC SURFACE STRUCTURE AT THE SOLID-VACUUM AND SOLID-GAS INTERFACES

Most of the surface structure determinations are carried out at these interfaces because of the availability of experimental techniques that can be applied to them. Low energy electron diffraction surface crystallography provided most of the available surface structure data<sup>4</sup>, although other techniques including electron microscopy, ion scattering, field ion microscopy, synchrotron based techniques (EXAFS and photo electron diffraction) and most recently the STM and the AFM have also contributed in significant ways. Measurement of the intensities of back-diffracted low energy (10-200 eV) electron beams provides the essential data to determine the location of surface atoms and the location of atoms in the top 3-5 layers near the surface. Great improvements in detector technology (resistive anode, channel plate) permits us to determine the surface structures of disordered monolayers on single crystal surfaces also and the use of low incident electron beam intensities ( $\sim 10^{-9}$  amp/ $\text{mm}^2$ ) to avoid electron beam damage of the surface. Improvements of the multiple scattering theory of LEED in the form of tensor-LEED allows the determination of the surface structure of more complex systems involving many atoms at different surface sites. Let us review what we learned about the atomic structure at the a) solid vacuum and b) solid-gas interfaces.

### (a) Surface structure at the solid-vacuum interface

The old heterogeneous rigid lattice model of the solid-vacuum interface is shown in Figure 1. This model was developed in the 1950's when electron microscopy and field ion microscopy studies revealed the presence of steps and kinks at surfaces of ionic crystals and transition metals<sup>5</sup>. It was assumed that the surface atoms occupy equilibrium positions that are the same as for atoms in the bulk. Thus, by knowing the bulk structure the location of the surface atoms can be predicted even at the step and kink sites.

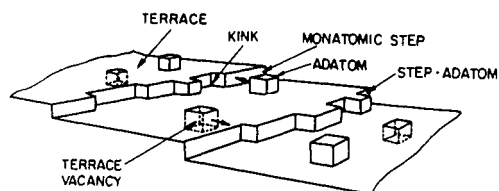


Fig. 1. The rough-rigid-surface model



Fig. 2. Shortened interlayer spacing between the first and second layer of atoms at the surface.

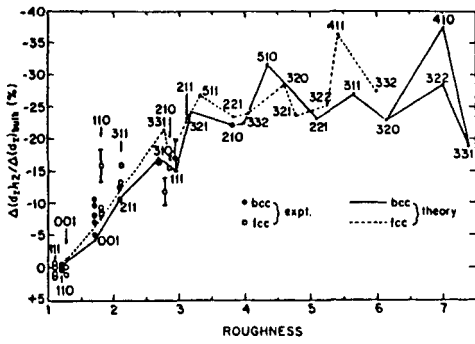


Fig. 3. Percent contraction as a function of surface roughness (1/packing density) for a large number of metal crystal surfaces.

This model has been found to be erroneous by LEED surface crystallography studies. The interlayer spacing between the first and second layer is contracted significantly (Figure 2). The contraction is larger the more open the surface is. By plotting the percent contraction indicated by the negative values as a function of surface roughness<sup>6</sup> (defined as 1/packing density) one can see how the reduction in interlayer spacing becomes larger for more open rougher surfaces as shown in Figure 3. There are steps and kinks in these contracted surface layers but the magnitude of contraction is very large at these sites leading to a smoothing and restructuring at these defect sites on the atomic scale. Thus the equilibrium positions of surface atoms are very different from those predicted by the rigid lattice model.

The inward relocation of surface atoms often lead to surface reconstruction. That is the surface atoms produce long range ordered structures with unit cells that are very different from the projection of the bulk unit cell to that surface. The Si(100)·(2x1) and the Pt(100)·(1x5) surface structures<sup>7,8</sup> were among the first where the location of surface atoms have been determined Figure 4a and 4b. We show the SiC(100) reconstructed

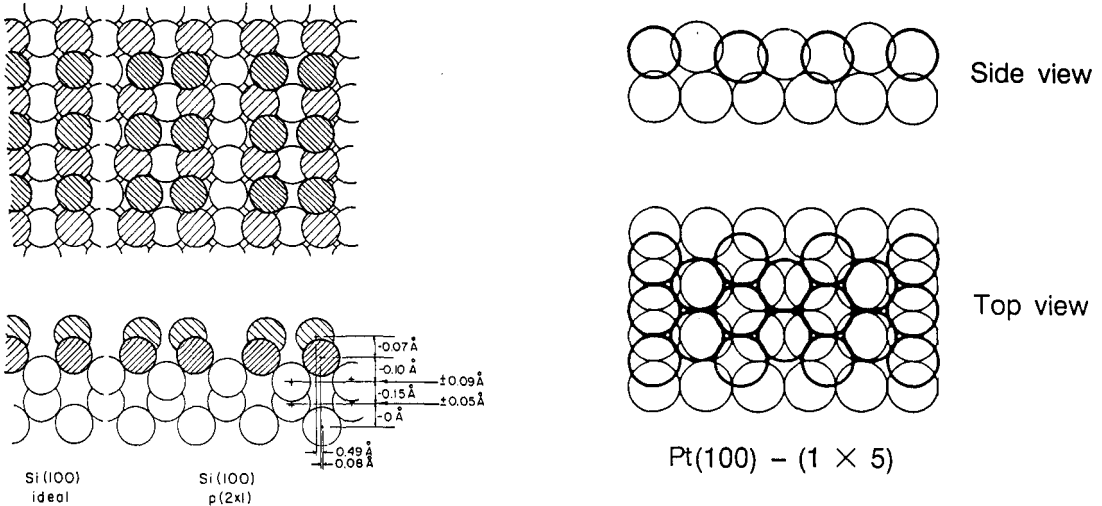


Fig. 4. a) The Si(100)-(2x1) reconstructed surface.

b) The Pt(100)-(1x5) reconstructed surface.

surface structure that we determined recently<sup>9</sup>. This surface is terminated either by silicon atoms or by carbon atoms. Both silicon and carbon terminated surfaces are reconstructed with respect to the structure of silicon carbide in the bulk (Figures 5a and 5b).

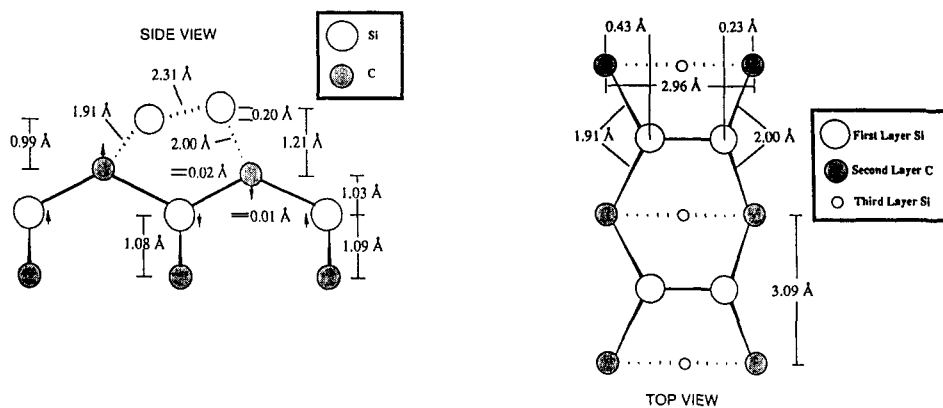


Fig. 5. a) The best fit surface structure for the  $\beta$ -SiC(100)-(2x1) surface in top view and side view. (Note: distances are not to scale.)

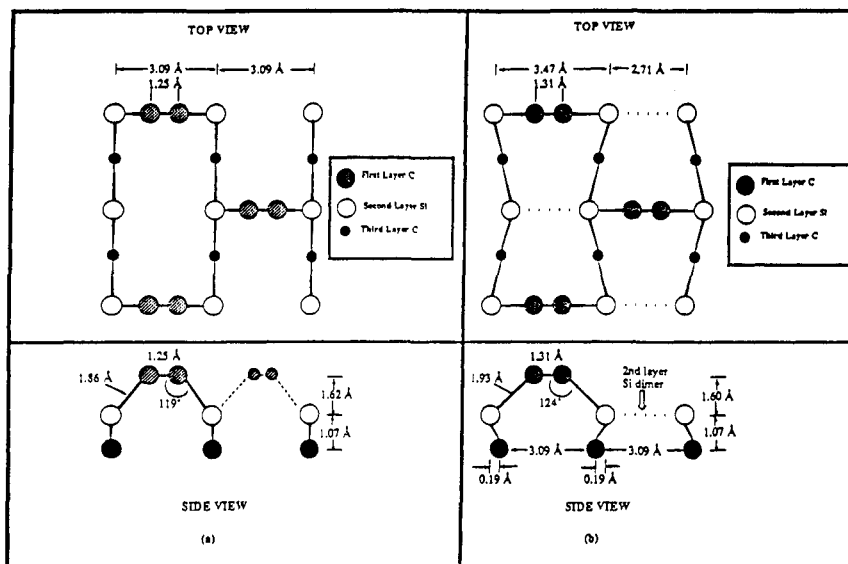
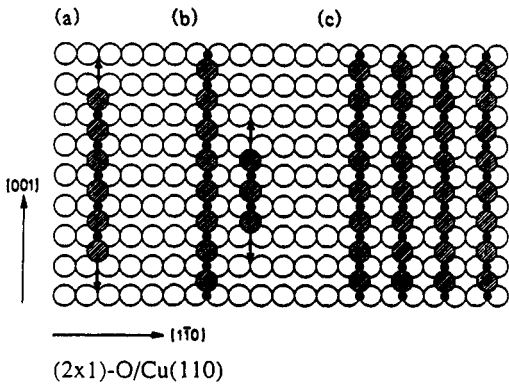


Fig. 5 b) The best fit surface structure for the c(2x2) surface produced by (i) exposure of the (2x1) to 100 Langmuir of  $C_2H_4$  at 1125 K and (ii) annealing the (2x1) at 1300 K in UHV for 10-15 min. The two preparations lead to closely similar structures, whose differences may be due to hydrogen left over from treatment (i).

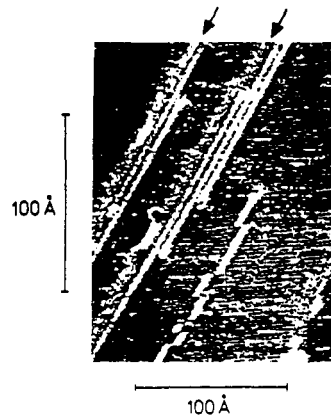
### (b) Surface structure at the solid-gas interface

When a monolayer of atoms or molecules chemisorb on a transition metal or semiconductor surface it was assumed that the substrate atoms move back to their bulk like positions from the relaxed inward equilibrium positions when clean. This assumption was maintained until recently. This is not what happens however has been shown by LEED surface crystallography. As a consequence of forming new chemical bonds with the chemisorbed atoms or molecules the surface atoms move into new positions but they are very different from the bulklike sites. This is called adsorbate induced restructuring<sup>10</sup>. We discuss two examples reported recently: Oxygen on Cu(110) and ethylene on Rh(111) single crystal surfaces.

The chemisorption of oxygen on the (110) crystal face of copper produces a new surface unit cell<sup>11</sup>. LEED surface crystallography studies indicate that the surface reconstructs and the new surface structure which is the mixed oxygen copper lattice is shown in Figure 6. STM studies can also monitor the dynamics of restructuring as the patches of restructured<sup>11</sup> copper surface grows at the expense of the unreconstructed copper domains<sup>12</sup>. Table 2 lists many of the surface structures that form as a result of



D.J.Coulman, J.Wintterlin, R.J.Behm and G.Ertl.  
Phys. Rev. Lett. **64** (1990) 1761



STM image of (2x1)O nuclei in different growth phases: two nuclei two and three rows wide, respectively, at the upper edge of steps along [001] and a single-row nucleus on the flat terrace. Step edges are marked by arrows.

Fig. 6. Oxygen chemisorption induced restructuring of the Cu(110) crystal face.

adsorbate induced restructuring, carbon hydrogen, sulfur, in addition to oxygen restructures completely the substrate surface when they adsorb. When the chemisorbed layer is removed by a chemical reaction or by heat treatments the original relaxed clean surface structure is usually regenerated.

Another example of adsorbate induced restructuring is revealed by a recent study of ethylene adsorption on Rh(111)<sup>13</sup>. This molecule forms ethylidyne species on many transition metals near 300K including rhodium. Its molecular structure is C<sub>2</sub>H<sub>3</sub>, with its C-C bond stretched to almost a single bond -1.45Å and lined up perpendicular to the metal surface<sup>14</sup>. Recent tensor-LEED calculations that are sensitive to changes in the metal-metal distances in the surface revealed the surface structure as shown in Figure 7a and 7b. Bonding with the carbon atom increases the metal-metal distances which forces a displacement in the substrate pushing the metal atom next to the metal-carbon bond deeper into the surface. Thus the metal surface becomes ruffled exhibiting atomic scale corrugation. The metal atom in the second layer right under the adsorption site of the organic molecule moves upward thus providing four metal carbon bonds instead of three for optimum bonding strength.

Different ethylidyne species: bond distances and angles  
r<sub>C</sub> = carbon covalent radius, r<sub>M</sub> = bulk metal atomic radius

	C (Å)	m	r <sub>M</sub>	r <sub>C</sub>	α (°)
Co <sub>3</sub> (CO) <sub>9</sub> CCH <sub>3</sub>	1.53 (3)	1.90 (2)	1.25	0.65	131.3
H <sub>3</sub> Ru <sub>3</sub> (CO) <sub>9</sub> CCH <sub>3</sub>	1.51 (2)	2.08 (1)	1.34	0.74	128.1
H <sub>3</sub> Os <sub>3</sub> (CO) <sub>9</sub> CCH <sub>3</sub>	1.51 (2)	2.08 (1)	1.35	0.73	128.1
Pf (111) + (2 x 2) CCH <sub>3</sub>	1.50	2.00	1.39	0.61	127.0
Rh (111) + (2 x 2) CCH <sub>3</sub>	1.45 (10)	2.03 (7)	1.34	0.69	130.2
H <sub>3</sub> C - CH <sub>3</sub>	1.54			0.77	109.5
H <sub>2</sub> C = CH <sub>2</sub>	1.33			0.68	122.3
HC ≡ CH	1.20			0.60	180.0

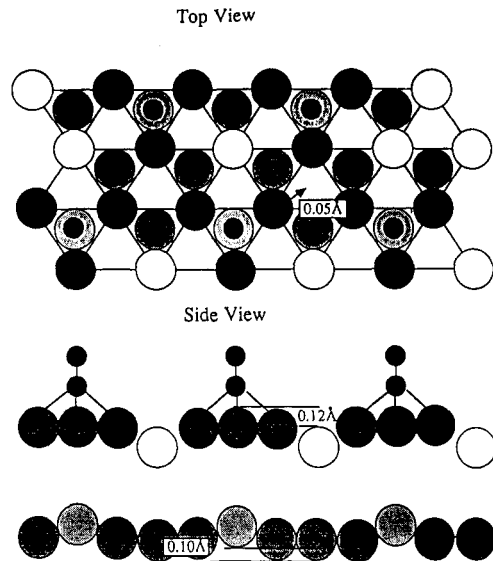


Fig. 7. a) The ethylidyne molecular surface structure  
b) The restructuring of the Rh(111) crystal face induced by ethylidyne chemisorption.

It should be noted that the (111) crystal face is the closest packed surface for face centered cubic solids. If this surface restructures the more open crystal faces (rougher surfaces) will restructure even more dramatically for thermodynamic reasons. The driving force for restructuring is the formation of such strong adsorbate-substrate bonds that their formation pays for the energy input necessary to weaken the metal-metal bonds at the surface as the metal atoms move into new equilibrium position. The less nearest neighbor metal atoms are (the more open is the surfaces) the less energy has to be expended to move the surface atoms into new equilibrium positions as the adsorbate-substrate bonds formed.

As these two examples indicate adsorbate induced restructuring can occur on the time scale of chemisorption probably within  $10^{-12}$ - $10^{-9}$  seconds. Recent studies indicate that surface restructuring occurs also on the time scale of catalytic reactions,  $10^{-3}$ -1 sec. CO oxidation and other surface reactions often exhibit oscillation in certain ranges of reactant partial pressures and temperatures<sup>15</sup>. It has been possible to monitor the periodic restructuring of these surfaces that occurs with the same frequency as the reaction rate oscillations<sup>16</sup>.

Adsorbate induced restructuring is also responsible for changes of particle size and shape that occur by atom transport over longer periods ( $1-10^4$  sec). Adsorbates often stabilize certain crystal faces by forming strong chemical bonds with that particular surface that would not be thermodynamically stable in solid vapor equilibrium in the absence of the impurity or adsorbate. When adsorbates of this type are added to surfaces they are called structural promoters if the surface they stabilize is chemically active (for example the alumina stabilized iron (111) crystal face for ammonia synthesis). They are called poisons or inhibitors if the surface they stabilize is chemically inactive (for example the sulfur stabilized (100) face of nickel).

#### INFLUENCE OF ADSORBATE INDUCED RESTRUCTURING ON CHEMISORPTION BOND AT HIGH COVERAGES

Studies of surface structure at high coverages are especially important because high surface coverages are produced when the solid surface functions under high gas pressures or in contact with a liquid. Studies of the chemisorption bond as a function of coverage revealed a marked decrease in the heat of adsorption above 50% of a monolayer coverage for most chemisorbed systems with a single adsorbate<sup>17</sup>. This was interpreted as due to repulsive adsorbate-adsorbate interactions as the adsorbed atoms or molecules are pushed closer together. Alkali metal ions neutralized to form atomic layers with much weaker surface bonds than the ions that exist at low coverages. This occurs with increasing coverage. The heat of adsorption of carbon monoxide near one monolayer becomes about 1/3 of its low coverage (10% coverage) value on most transition metal surfaces<sup>18</sup>.

However, adsorbate induced restructuring of the substrate can turn the repulsive to attractive interaction as the coverage increases. This is shown for sulfur chemisorption on the (0001) crystal face of rhenium<sup>19</sup>. At low coverages the sulfur atoms occupy 3-fold sites that can be studied both by LEED surface crystallography and by STM. The surface metal atoms move into new equilibrium positions exhibiting adsorbate induced restructuring that has important consequences as the coverage of sulfur increases. Instead of the expected repulsive sulfur-sulfur interaction, sulfur condenses to form trimers then tetramers and hexamers with increasing coverage. These sulfur aggregates show sulfur-sulfur bond distances that are similar to the metal-metal distances in the rhenium substrate. They are also ordered aggregates as shown in the pictures obtained in ultra high vacuum by STM in Figures 8a, 8b, 8c and 8d. It appears that adsorbate induced restructuring transformed the usually repulsive adsorbate-adsorbate interaction to become attractive causing sulfur aggregation.

Sulfur monolayers have important applications as lubricants. STM studies indicate that the sulfur aggregate covered metal surface becomes more elastic, the tunneling tip can penetrate deeper into the surface without causing irreversible structural damage as was observed in the absence of sulfur.

#### CO-ADSORPTION MONOLAYER STRUCTURES

The coadsorption of two different molecules can lead to the formation of ordered monolayer structures where both molecules are part of the unit cell<sup>20</sup>. Figure 9 shows the CO-C<sub>2</sub>H<sub>2</sub> coadsorbed surface structure and Figure 10 shows the carbon monoxide - benzene coadsorbed structure<sup>21</sup>. Ordering is observed if one of the adsorbates is an electron donor to the metal surface (organic molecules are usually electron donors)

while the other molecule is an electron acceptor (CO on Rh). If two donors or two acceptors are coadsorbed phase separation into islands of one type of molecule or the other type is frequently observed.

The coadsorption phenomenon is further complicated by adsorbate induced restructuring. So far none of the coadsorbed surface structures that have been reported have been analyzed by taking into account surface restructuring.

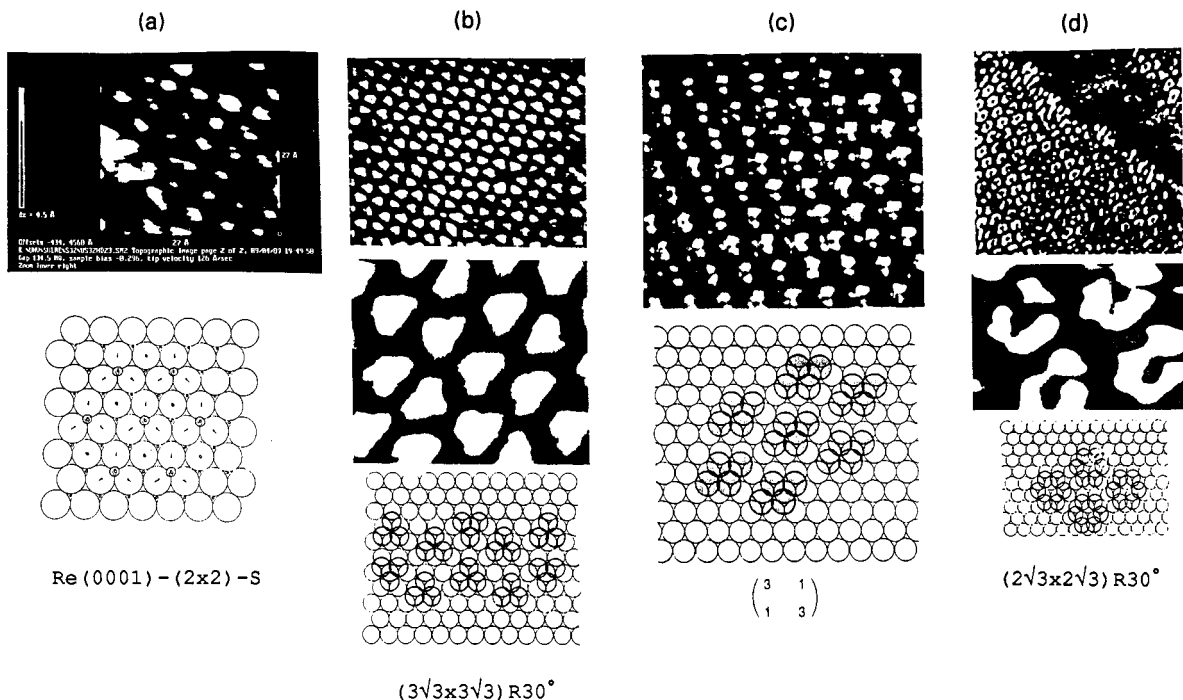


Fig. 8. Scanning tunneling microscopy and real space structures of sulfur on Re(0001) crystal face as a function of coverage a) monomer, b) trimer, c) tetramer and d) hexamer.

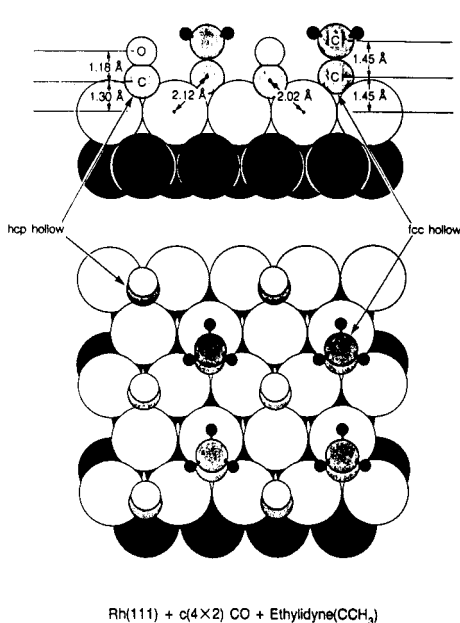


Fig. 9. The CO-C<sub>2</sub>H<sub>3</sub> co-adsorbed surface structure on Rh(111).

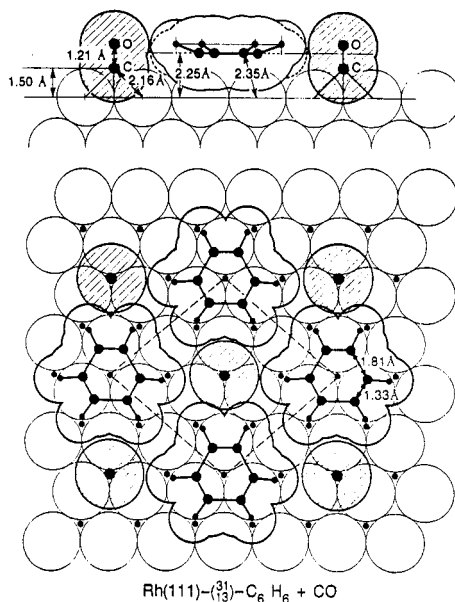


Fig. 10 Carbon monoxide benzene coadsorbed structure.

## THE FRONTIERS OF MONOLAYER STRUCTURE ANALYSIS

All the examples that I have given above come from atomic scale studies of monolayer structures at the solid-vacuum and solid-gas interfaces. There are a few studies of monolayer structures at the liquid-gas interface. For example, using non linear laser optics<sup>22</sup>, SFG detects OH vibrational spectra at the water air interface indicating that the water molecules are aligned there with their OH groups perpendicular to the liquid surface. When alcohol is added to water the OH spectrum disappears indicating the surface segregation of the alcohol molecules and the formation of hydrogen bonds at the liquid interface. However, investigations of liquid-gas interfaces are in their infancy.

The buried interfaces solid-solid or solid-liquid are most important in many interface based technologies including the formation of coatings, magnetic and semiconductor thin films. Figure 11 shows a semiconductor heterojunction imaged by electron microscopy. We should be able to determine the atomic arrangements at both sides of the interface. These studies have not been performed as yet. When a monolayer of molecules is sandwiched between the solids it is the type of interface structure encountered in boundary layer lubrication. Studies of this type of systems are in progress in my laboratory. It would be essential to investigate the molecular structure of the buried interface that is in relative motion (tribology). This requires dynamic surface analysis techniques giving time resolved information on time scales that are short as compared to the times of the lateral motion of the two interfaces relative to each other. It is hoped that such studies will be carried out in the near future.

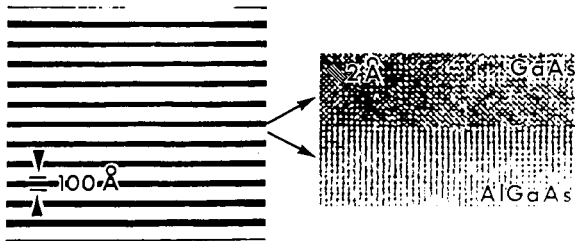


Fig. 11. Semiconductor heterojunction.

The studies of small atomic aggregates, clusters are just beginning as well. These clusters may be catalysts on high surface area supports. They could be colloids or made of carbon, metals or semiconductors. New synthetic methods using reverse micelles or laser evaporation can produce clusters of all the same particle size that can be varied in the  $10^{-10}$  Å ranges. These are likely to have interesting surface structures that may be fluxional as many different shapes may have similar thermodynamic stabilities. These systems are also at the frontiers of surface structure analysis.

### Acknowledgement

This work was supported by the Director, Office of Energy Research, Office of Basic Energy Sciences, Materials Sciences Division, U.S. Department of Energy under Contract No. DE-AC03--76SF00098.

### REFERENCES

1. I. Langmuir and J.A. Orange, *Trans Am. Inst. of Electrical Engineers* 37, 1913 (1913)
2. I. Langmuir, *J. Am. Chem. Soc.* 39, 1848 (1917)
3. V.K. La Mer Ed. "Retardation of Evaporation by Monolayers, Academic Press, N.y. 1962
4. S.W. Wang, D.F. Ogletree, M.A. Van Hove and G.A. Somorjai, *Adv. in Quantum Chem.*, 20, 2-147 (1989)
5. *Chemistry in Two Dimensions: Surfaces*, Book, Cornell University Press, 1981
6. F. Jona and P.M. Marcus, "The Structure of Surfaces II"; Springer Verlag: Berlin 1988; page 90
7. J.A. Appelbaum and D.R. Hamann, *Surf. Sci.* 74, 21 (1978)
8. M.A. Van Hove, R.J. Koestner, P.C. Stair, J.P. Biberian, L.L. Kesmodel and G.A. Somorjai; *Surf. Sci.* 103, 189 (1981)



9. J.Powers, A. Wander, M.A. Van Hove, submitted Surf. Sci. (1991)
10. G.A. Somorjai and M.A. Van Hove, Cat. Letts. 1, 433 (1988)
11. C. Woell, R.J. Wilson, S. Chang, H.C. Zeng and K.A.R. Mitchell, Phys. Rev. B 42, 11926 (1990)
- 11a. G. Ertl, Surf. Sci. 6, 208 (1967)
12. D.J. Coulman, J. Wintterlin, R.J. Behum and G. Ertl, Phys. Rev. Lett. 64, 1761 (1990); and S.R. Parkin, H.C. Zeng, M.Y. Zhou and K.A.R. Mitchell, Phys. Rev. B41, 5432 (1990)
13. A. Wander, M.A. Van Hove and G.A. Somorjai, accepted Phys. Rev. Lett. (1991)
14. R.J. Koestner, M.A. Van Hove and G.A. Somorjai, Surf. Sci. 121, 321 (1982)
15. G. Ertl, Ber. Buns. Phys. Chem. 90, 284 (1986)
16. R.C. Yeates, J.E. Turner, A.J. Gellman, and G.A. Somorjai, Surf. Sci. 149, 175 (1985)
17. E.L. Garfunkel and G.A. Somorjai, in: Alkali Adsorption on Metals and Semiconductors (Elsevier, 1989) pg. 319 Ed. H. Bonzel
18. H. Conrad, G. Ertl, J. Koch and E.E. Latta, Surf. Sci. 43 (1974) 462
19. D.F. Ogletree, R.Q. Hwang, D.M. Zeglinski, A. Lopez Vazquez-de-Parga, M. Salmeron and G.A. Somorjai, JVST (B), 9 (2), 886 (1991)
20. C.M. Mate, C.T. Kao and G.A. Somorjai, Surf. Sci. 206 (1988) 145
21. H. Ohtani, M.A. Van Hove and G.A. Somorjai, Appl. Surf. Sci. 33-4, 254-260 (1988)
22. R.Y. Shen, Nature, 337 (1989) 6207

Table 1 - Surface Science Techniques That Are Used Frequently

NAME	ACRONYM	DESCRIPTION	PRIMARY SURFACE INFORMATION
Adsorption or Selective Chemisorption	Adsorption	Atoms or molecules are physisorbed, and their concentration measures total surface area. Chemisorption of atoms or molecules on sites yields surface concentration of selected elements or atomic sites.	surface area site concentration composition
Atom or Helium Diffraction	AD	Monoenergetic beams of thermal energy neutral atoms are elastically scattered off ordered surfaces and detected as a function of scattering angle. This gives structural information on the outermost layer of the surface. Atom diffraction is extremely sensitive to surface ordering and defects.	atomic structure
Auger Electron Appearance Potential Spectroscopy	AEPS	The AEAPS cross-section is monitored by Auger electron intensity. Also known as APAES.	electronic structure
Auger Electron Spectroscopy	AES	Core-hole excitations are created, usually by 1-10 KeV incident electrons, and Auger electrons of characteristic energies are emitted through a two-electron process as excited atoms decay to their ground state. AES gives information on the near-surface chemical composition.	composition

Table 1 (contd.)

NAME	ACRONYM	DESCRIPTION	PRIMARY SURFACE INFORMATION
Atomic Force Microscopy	AFM	Similar to STM. An extremely delicate mechanical probe is used to scan the topography of a surface by measuring forces exerted by surface atoms. Light interference is used to measure the deflection of the mechanical surface probe. This is designed to provide STM-type images of insulating surfaces or to detect mechanical properties at the molecular level.	atomic structure
Appearance Potential Auger Electron Spectroscopy	APAES	See AEAPS	
Appearance Potential X-ray Photoemission Spectroscopy	APXPS	The EAPFS excitation cross-section is monitored by fluorescence from core-hole decay (also known as SXAPS).	electronic structure
Angle-Resolved Auger Electron Spectroscopy	ARAES	Auger electrons are detected as a function of angle to provide information on the spatial distribution or environment of the excited atoms (see AES).	composition
Angle-Resolved Photo-Emission Fine Structure	ARPEFS	Electrons are detected at given angles after being photoemitted by polarized synchrotron radiation. The interference in the detected photoemission intensity as a function of electron energy ~100-500 eV above the excitation threshold gives structural information.	electronic structure
Angle-Resolved Photo-Emission Spectroscopy	ARPES	A general term for structure-sensitive photoemission techniques including ARPEFS, ARXPS, ARUPS, and ARXPD.	electronic structure
Angle-Resolved Ultraviolet Photoemission Spectroscopy	ARUPS	Electrons photoemitted from the valence and conduction bands of a surface are detected as a function of angle. This gives information on the dispersion of these bands (which is related to surface structure), and also structural information from the diffraction of the emitted electrons.	valence band structure
Angle-Resolved X-ray Photoemission Diffraction	ARXPD	Similar to ARXPS and ARPEFS. The angular variation in the photoemission intensity is measured at a fixed energy above the excitation threshold to provide structural information.	electronic structure
Angle-Resolved X-ray Photoemission Spectroscopy	ARXPS	The diffraction of electrons photoemitted from core levels gives structural information on the surface.	electronic structure
Conversion-Electron Mössbauer Spectroscopy	CEMS	A surface-sensitive version of Mössbauer spectroscopy. Like Mössbauer spectroscopy, this technique is limited to some isotopes of certain metals. After a nucleus is excited by $\gamma$ -ray absorption, it can undergo inverse $\beta$ -decay, creating a core hole. The decay of core holes by Auger processes within an electron mean free path of the surface produces a signal. Detecting emitted electrons as a function of energy gives some depth-profile information, because of the changing electron mean-free path.	oxidation state

Table 1 (contd.)

NAME	ACRONYM	DESCRIPTION	PRIMARY SURFACE INFORMATION
Dis-Appearance Potential Spectroscopy	DAPS	The EAPFS cross section is monitored by variations in the intensity of electrons elastically back-scattered from the surface.	electronic structure
Electron Appearance Potential Fine-Structure	EAPFS	A fine-structure technique (see EXAFS). Core holes are excited by monoenergetic electrons at ~1 eV. The modulation in the excitation cross section may be monitored through adsorption, fluorescence, or Auger emission.	atomic structure
Electron-Energy-Loss Near-Edge Structure	ELNES	Similar to NEXAFS, except monoenergetic high-energy electrons ~60-300 KeV excite core holes.	atomic structure
Electron-Energy-Loss Spectroscopy	ELS	Monoenergetic electrons ~5-50 eV are scattered off a surface and the energy losses are measured. This gives information on the electronic excitations of the surface and adsorbed molecules (see HREELS). Sometimes called EELS.	electronic structure
Electron Spectroscopy for Chemical Analysis	ESCA	Now generally called XPS.	composition, oxidation state
Electron-Stimulated Ion Angular Distribution	ESDIAD	Electrons break chemical bonds in adsorbed atoms or molecules, causing ionized atoms or radicals to be ejected from the surface along the axis of the broken bond by Coulomb repulsion. The angular distribution of these ions gives information on the bonding geometry of adsorbed molecules.	molecular orientation
Extended X-ray Adsorption Fine Structure	EXAFS	Monoenergetic photons excite a core hole. The modulation of the adsorption cross-section with energy 100-500 eV above the excitation threshold yields information on the radial distances to neighboring atoms. The cross section can be monitored by fluorescence as core holes decay or by the attenuation of the transmitted photon beam. EXAFS is one of many "fine-structure" techniques.	local atomic structure coordination no.
Extended X-ray Energy Loss Fine Structure	EXELFS	A fine-structure technique similar to EXAFS, except that 60-300 eV electrons rather than photons excite core holes.	atomic structure
Field-Ionization Microscopy	FIM	A strong electric field-volts/Angstrom is created at the tip of a sharp, single-crystal wire. Gas atoms, usually He, are polarized and attracted to the tip by the strong electrostatic field, and then ionized by electrons tunneling from the gas atoms into the tip. These ions, accelerated along radial trajectories by Coulomb repulsion, map out the variations in the electric-field strength across the surface with atomic resolution, showing the surface topography.	atomic structure and surface diffusion

Table 1 (contd.)

NAME	ACRONYM	DESCRIPTION	PRIMARY SURFACE INFORMATION
Fourier-Transform Infra-Red Spectroscopy	FTIR	Broad-band IRAS experiments are performed, and the IR adsorption spectrum is deconvoluted by using a Doppler-shifted source and the Fourier analysis of the data. This technique is not restricted to surfaces.	molecular structure
High-Energy Ion Scattering	HEIS	High-energy ions, above ~500 KeV, are scattered off of a single-crystal surface. The "channeling" and "blocking" of scattered ions within the crystal can be used to triangulate deviations from the bulk structure. HEIS has been especially used to study surface reconstructions and the thermal vibrations of surface atoms (See also MEIS, ISS.)	atomic structure
High-Resolution Electron-Energy-Loss Spectroscopy	HREELS	A monoenergetic electron beam, usually ~ 2-10 eV, is scattered off a surface, and energy losses below ~ 0.5 eV to bulk and surface phonons and vibrational excitations of adsorbates are measured as a function of angle and energy (also called EELS).	molecular structure
Ion-Neutralization Spectroscopy	INS	Slow ionized atoms, typically He <sup>+</sup> , are incident on a surface where they are neutralized in a two-electron process that can eject a surface electron, a process similar to Auger emission from the valence band. The ejected electrons are detected as a function of energy, and the surface density of states can be determined from the energy distribution. The interpretation of the data is more complicated than for SPI or UPS.	valence band
Infrared Reflection Adsorption Spectroscopy	IRAS	Monoenergetic IR photons are reflected off a surface, and the attenuation of the IR intensity is measured as a function of frequency. This yields a spectrum of the vibrational excitations of adsorbed molecules. Recent improvements in the sensitivity of this technique allow IRAS measurements to be made on single-crystal surfaces.	molecular structure
Infra-Red Emission Spectroscopy	IRES	The vibrational modes of adsorbed molecules on a surface are studied by detecting the spontaneous emission of infrared radiation from thermally excited vibrational modes as a function of energy.	molecular structure
Ion-Scattering Spectroscopy	ISS	Ions are inelastically scattered from a surface, and the chemical composition of the surface is determined from the momentum transfer to surface atoms. The energy range is ~ 1 KeV to 10 MeV, and the lower energies are more surface sensitive. At higher energies this technique is also known as Rutherford Back-Scattering (RBS).	composition
Low-Energy Electron Diffraction	LEED	Monoenergetic electrons below ~ 500 eV are elastically back-scattered from a surface and detected as a function of energy and angle. This gives information on the structure of the near surface region.	atomic structure and molecular structure

Table 1 (contd.)

NAME	ACRONYM	DESCRIPTION	PRIMARY SURFACE INFORMATION
Low-Energy Ion Scattering	LEIS	Low-energy ions, below ~ 5 eV, are scattered from a surface, and the ion "shadowing" gives information on surface structure. At these low energies the surface-atom ion-scattering cross section is very large, resulting in large surface sensitivity. Accuracy is limited because the low-energy ion-scattering cross sections are not well known.	atomic structure
Low-Energy Positron Diffraction	LEPD	Similar to LEED with positrons as the incident particle. The interaction potential for positrons is somewhat different than for electrons, so the form of the structural information is modified.	atomic structure
Medium-Energy Electron Diffraction	MEED	Similar to LEED, except the energy range is higher, ~ 300-1000 eV.	atomic structure
Medium-Energy Ion Scattering	MEIS	Similar to HEIS, except that incident ion energies are ~ 50-500 KeV.	atomic structure
Neutron Diffraction		Neutron diffraction is not an explicitly surface-sensitive technique, but neutron diffraction experiments on large surface-area samples have provided important structural information on adsorbed molecules, and also on surface phase transitions.	molecular structure
Near-Edge X-ray Adsorption Fine Structure	NEXAFS	A core-hole is excited as in fine structure techniques (see EXAFS), except the fine structure within ~ 30 eV of the excitation threshold is measured. Multiple scattering is much stronger at low electron energies, so this technique is sensitive to the local 3-dimensional geometry, not just the radial separation between the source atom and its neighbors. The excitation cross section may be monitored by detecting the photoemitted electrons or the Auger electrons emitted during the core-hole decay.	atomic structure
Nuclear Magnetic Resonance	NMR	NMR is not an explicitly surface-sensitive technique, but NMR data on large surface-area samples ( $\geq 1\text{m}^2$ ) have provided useful data on molecular adsorption geometries. The nucleus magnetic moment interacts with an externally applied magnetic field and provides spectra highly dependent on the nuclear environment of the sample. The signal intensity is directly proportional to the concentration of the active species. This method is limited to the analysis of magnetically active nuclei.	molecular structure
Normal Photoelectron Diffraction	NPD	Similar to ARPEFS with a somewhat lower energy range.	atomic structure
Rutherford Back-Scattering	RBS	Similar to ISS, except the main focus is on depth-profiling and composition. The momentum transfer in back-scattering collisions between nuclei is used to identify the nuclear masses in the sample, and the smaller, gradual momentum-loss of the incident nucleus through electron-nucleus interactions provides depth-profile information	composition

Table 1 (contd.)

NAME	ACRONYM	DESCRIPTION	PRIMARY SURFACE INFORMATION
Reflection High-Energy Electron Diffraction	RHEED	Monoenergetic electrons of ~ 1-20 KeV are elastically scattered from a surface at glancing incidence, and detected as a function of angle and energy for small forward-scattering angles. Back-scattering is less important at high energies, and glancing incidence is used to enhance surface sensitivity.	atomic structure
Surface Electron-Energy-Loss Fine Structure	SELEFS	A fine-structure technique similar to EXELFS, except the incident electron is more surface sensitive because of the lower excitation energy.	atomic structure
Surface-Enhanced Raman Spectroscopy	SERS	Some surface geometries (rough surfaces) concentrate the electric fields of Raman scattering cross section so that it is surface sensitive. This gives information on surface vibrational modes, and some information on geometry via selection rules.	molecular structure
Surface-Extended X-ray Adsorption Fine-Structure	SEXAFS	A more surface-sensitive version of EXAFS where the excitation cross-section fine structure is monitored by detecting the photoemitted electrons (PE-SEXAFS), Auger electrons emitted during core-hole decay (Auger-SEXAFS), or ions excited by photoelectrons and desorbed from the surface (PSD-SEXAFS).	atomic structure
Sum Frequency Generation	SFG	Similar to SHG. One of the lasers has a tuneable frequency that permits variation of the second harmonic signal. In this way the vibrational excitation of adsorbed molecules is achieved.	molecular structure
Second-Harmonic Generation	SHG	A surface is illuminated with a high-intensity laser, and photons are generated at the second-harmonic frequency through nonlinear optical process. For many materials only the surface region has the appropriate symmetry to produce an SHG signal. The nonlinear polarizability tensor depends on the nature and geometry of adsorbed atoms and molecules.	electronic structure, molecular orientation
Secondary-Ion Mass Spectroscopy	SIMS	Ions and ionized clusters ejected from a surface during ion bombardment are detected with a mass spectrometer. Surface chemical composition and some information on bonding can be extracted from SIMS ion fragment distributions.	composition
Surface Penning Ionization	SPI	Neutral atoms, usually He, in excited states are incident on a surface at thermal energies. A surface electron may tunnel into the unoccupied electronic level, causing the incident atom to become ionized and eject an electron, which is then detected. This technique measures the density of states near the Fermi-level, and is highly surface sensitive.	electronic structure
Spin-Polarized Low-Energy Electron Diffraction	SPLEED	Similar to LEED, except the incident electron beam is spin-polarized. This is particularly useful for the study of surface magnetism and magnetic ordering.	magnetic structure

Table 1 (contd.)

NAME	ACRONYM	DESCRIPTION	PRIMARY SURFACE INFORMATION
Scanning Tunneling Microscopy	STM	The topography of a surface is measured by mechanically scanning a probe over a surface with Angstrom resolution. The distance from the probe to the surface is measured by the probe-surface tunneling current. Also known as Scanning Electron Tunneling Microscopy (SETM).	atomic structure
Soft X-ray Appearance Potential Spectroscopy	SXAPS	Another name for APXPS.	
Transmission Electron Microscopy	TEM	TEM can provide surface information for carefully prepared and oriented bulk samples. Real images have been formed of the edges of crystals where surface planes and surface diffusions have been observed. Diffraction patterns of reconstructed surfaces, superimposed on the bulk diffraction pattern, have also provided surface structural information.	atomic structure
Thermal-Desorption Spectroscopy	TDS	An adsorbate-covered surface is heated, usually at a linear rate, and the desorbing atoms or molecules are detected with a mass spectrometer. This gives information on the nature of adsorbate species and some information on adsorption energies and the surface structure.	composition, heat of adsorption, surface structure
Temperature-Programmed Desorption	TPD	Similar to TDS, except the surface may be heated at a nonuniform rate to obtain more selective information on adsorption energies.	composition, heat of adsorption
Ultraviolet Photoemission Spectroscopy	UPS	Electrons photoemitted from the valence and conduction bands are detected as a function of energy to measure the electronic density of states near the surface. This gives information on the bonding of adsorbates to the surface (see ARUPS).	valence band structure
Work-Function Measurements	WF	Changes in the work function during the adsorption of atoms and molecules provide information on charge-transfer and chemical bonding.	electronic structure
X-ray Adsorption Near-Edge Structure	XANES	Another name for NEXAFS.	
X-ray Photoemission Spectroscopy	XPS	Electrons photoemitted from atomic core levels are detected as a function of energy. The shifts of core-level energies give information on the chemical environment of the atoms (see ARXPS, ARXPD).	composition, oxidation state
X-Ray Diffraction	XRD	X-ray diffraction has been carried out at extreme glancing angles of incidence where total reflection assures surface sensitivity. This provides structural information that can be interpreted by well-known methods. An extremely high x-ray flux is required to obtain useful data from single-crystal surfaces. Bulk x-ray diffraction is used to determine the structure of organo metallic clusters, which provide comparisons to molecules adsorbed on surfaces. X-ray diffraction has also given structural information on large surface-area samples.	atomic structure

Table 2: Adsorbate induced restructuring of metal and semiconductor surfaces

Surface-adsorbate system and periodicity	Method and reference of investigation	Type of restructuring
Cu(100)/O-(2* $\sqrt{2}$ x $\sqrt{2}$ )	LEED <sup>1</sup> STM/LEED <sup>2</sup> Theory (Effective Medium) <sup>3</sup>	Missing-row reconstruction Pairing of Ni-atoms next to row "Cu-O-Cu-chains" similar to Cu(110)
Ni(100)/C-p4g(2x2) Ni(100)/N-p4g(2x2)	LEED <sup>4</sup> SEXAFS <sup>5,6</sup>	4-fold site Clockwise rotation of 1 <sup>st</sup> layer atoms Buckling of 2 <sup>nd</sup> layer atoms
Ni(100)/Cl-c(2x2) Cu(100)/Cl-c(2x2) Mo(100)/C-c(2x2)	SEXAFS/XSW <sup>7</sup> SEXAFS <sup>8</sup> LEED <sup>45</sup>	4-fold site 1 <sup>st</sup> to 2 <sup>nd</sup> layer expansion
Cu(100)/N-c(2x2) Cu(100)/S-p(2x2)  Ni(100)/O-c(2x2) Ni(100)/O-p(2x2) Ni(100)/O-disordered Ni(100)/S-c(2x2) Ni(100)/S-p(2x2) Ni(100)/S-disordered	LEED <sup>9</sup> XRD <sup>10</sup> MEIS <sup>11</sup> LEED <sup>12</sup> LEED <sup>13,18</sup> LEED <sup>14,18</sup> DLEED <sup>15,18</sup> LEED <sup>16,18</sup> LEED <sup>17,18</sup> DLEED <sup>15,18</sup>	4-fold site 2 <sup>nd</sup> layer buckling (Atom underneath adsorbate moves down)
Cu(110)/K-(1x2) Cu(110)/Cs-(1x2)	LEED <sup>19</sup> LEED <sup>19</sup>	Low coverage induced missing-row reconstruction
Cu(110)/N-(2x3)	PED <sup>20</sup> LEIS <sup>21</sup> XPD/AES <sup>22</sup> STM <sup>23</sup>	Favoring "pseudo-square" model with square-like 1 <sup>st</sup> layer arrangement Favoring missing-row reconstruction with every 3 <sup>rd</sup> <110>-row missing
Cu(110)/O-(2x1)	SEXAFS <sup>24</sup> XRD <sup>25</sup> LEED <sup>26</sup> LEED <sup>27</sup> Theory (Effective Medium) <sup>3</sup> ICISS <sup>28</sup>	Missing-row reconstruction Long bridge site "Cu-O-Cu-chains" similar to Cu(100)
Ni(110)/O-(2x1)	LEED <sup>29</sup>	Missing-row reconstruction asymmetric long bridge site
Cu(110)/O-c(6x2)	STM/XRD <sup>30</sup>	Cu-atom c(6x2)-superstructure on (3x1) 2 per 3 missing-row reconstruction 2 oxygen sites
Ni(110)/H-(1x2)	LEED <sup>31</sup>	Row-pairing, 2 <sup>nd</sup> layer buckling
Ni(111)/O-(2x2)	LEED <sup>32</sup>	fcc-hollow site Clockwise rotation and buckling in 1 <sup>st</sup> layer
Ni(111)/O-p( $\sqrt{3}$ x $\sqrt{3}$ )	LEED <sup>33</sup>	fcc-hollow site
Ni(111)/S-(2x2)	LEED <sup>34</sup>	fcc-hollow site 1 <sup>st</sup> to 2 <sup>nd</sup> , 2 <sup>nd</sup> to 3 <sup>rd</sup> layer expansion
Rh(100)/O-(2x2)	LEED <sup>35</sup>	4-fold hollow site, layer contraction
Rh(110)/H	LEED <sup>36-41</sup>	5 superstructure phases Local outwards movement of substrate atoms with H-bond
Ru(001)/O-p(2x1)	LEED <sup>42</sup>	3-fold hcp-hollow site Buckling and row pairing in 1 <sup>st</sup> and 2 <sup>nd</sup> layer
Ru(001)/O-p(2x2)	LEED <sup>43</sup>	3-fold hcp-hollow site Buckling and lateral outwards movement in 1 <sup>st</sup> layer
Cr(110)/N-(1x1)	LEED <sup>44</sup>	4-fold hollow site 1 <sup>st</sup> layer expansion (24.8 %)
Mo(100)/S-c(2x2)	LEED <sup>45</sup>	4-fold hollow site 2 <sup>nd</sup> layer buckling
Rh(111)/C <sub>2</sub> H <sub>3</sub> -(2x2)	LEED <sup>47</sup>	Buckling in 1 <sup>st</sup> and 2 <sup>nd</sup> layer



Table 2 (contd.)

Surface-adsorbate system and periodicity	Method and reference of investigation	Type of restructuring
Si(100)/H-(2x1) Si(100)/F-(2x1) Si(100)/Cl-(2x1)	STM <sup>47</sup> LEIS <sup>48</sup> Theory (SLAB-MINDO) <sup>49</sup> ESDIAD <sup>50</sup> SEXAFS <sup>51</sup>	Dangling bond adsorption Dimer relaxation (lengthening)
Si(100)/O-(2x1)	SEXAFS <sup>52</sup> Theory (HF-Cluster) <sup>53</sup> Theory (DF-LDA) <sup>54</sup>	Dimer insertion (Adsorption into dimer and dimer lengthening)
Si(100)/K-(2x1) Si(100)/Na-(2x1) Si(100)/Li-(2x1)	LEED <sup>55</sup> SEXAFS <sup>56</sup> Theory (DF-LDA) <sup>57</sup> LEED <sup>58</sup> Theory (DF-LDA) <sup>59</sup>	One dimensional Alkali-chains Dimerization removed
Si(111)/Al-( $\sqrt{3}\times\sqrt{3}$ )R30° Si(111)/Ga-( $\sqrt{3}\times\sqrt{3}$ )R30° Si(111)/Sn-( $\sqrt{3}\times\sqrt{3}$ ) Ge(111)/Pb-( $\sqrt{3}\times\sqrt{3}$ )	LEED <sup>60</sup> Theory (Total energy) <sup>61</sup> LEED <sup>62</sup> STM <sup>63</sup> XSW, STM <sup>64</sup> XRD <sup>65</sup> LEED <sup>66</sup>	Removal of (7x7) T4-adsorption site (triangular site with 4-fold coordination)
Si(111)/B-( $\sqrt{3}\times\sqrt{3}$ )	XRD <sup>67</sup> LEED <sup>68</sup>	Removal of (7x7) T4-"upside down" site (triangular site with 4-fold coordination, B-Si substitution)
Si(111)/Fe-(1x1) Si(111)/As-(1x1) Si(111)/GaAs-(1x1)	LEED <sup>69</sup> XSW <sup>70</sup> MEIS <sup>71</sup> STM, MEIS <sup>72</sup> Theory (GVB) <sup>73</sup> XSW <sup>74</sup> Theory (DF-LDA) <sup>75</sup>	Removal of (7x7) Missing top layer in Fe-structure
Si(111)/Sb-( $\sqrt{3}\times\sqrt{3}$ ) Si(111)/Bi-( $\sqrt{3}\times\sqrt{3}$ )	XPD <sup>76</sup> XRD <sup>77</sup>	Removal of (7x7) Milk-stool structure Adsorbate trimers Si honeycomb layer on top in Bi-structure

## References for table 2:

- 1 H. C. Zeng, R. A. McFarlane and K. A. R. Mitchell, Surf. Sci. 208, L7 (1989)
- 2 Ch. Wöll, R. J. Wilson, S. Chiang, H. C. Zeng and K. A. R. Mitchell, Phys. Rev. B 42, 11926 (1990)
- 3 K. W. Jacobsen and J. K. Norskov, Phys. Rev. Lett. 65, 1788 (1990)
- 4 Y. Gauthier, R. Baudoing-Savois, K. Heinz and H. Landskron, Surf. Sci. in press (1991), Proceedings of ECOSS, Salamanca, Spain (1990)
- 5 L. Wenzel, D. Arvanitis, W. Daum, H. H. Rotermund, J. Stöhr, K. Baberschke and H. Ibach, Phys. Rev. B 36, 7689 (1987)
- 6 D. Arvanitis, K. Baberschke and L. Wenzel, Phys. Rev. B 37, 7143 (1988)
- 7 T. Yokoyama, Y. Takata, T. Ohta, M. Funagashi, Y. Kitajima and H. Kuroda, Phys. Rev. B 42, 7000 (1990)
- 8 J. R. Patel, D. W. Berreman, F. Sette, P. H. Citrin, J. E. Rowe, P. L. Cowan, T. Jack and B. Karlin, Phys. Rev. B 40, 1330 (1989)
- 9 H. C. Zeng and K. A. R. Mitchell, Langmuir 5, 829 (1989)
- 10 E. Vlieg, I. K. Robinson and R. McGrath, Phys. Rev. B 41, 7896 (1990)
- 11 Q. T. Jiang, P. Fenter and T. Gustafsson, Phys. Rev. B 42, 9291 (1990)
- 12 H. C. Zeng, R. A. McFarlane and K. A. R. Mitchell, Can. J. Phys. (1991), in press

- 13 W. Oed, H. Lindner, U. Starke, K. Heinz and K. Müller, *Surf. Sci.* 224, 179 (1989)
- 14 W. Oed, H. Lindner, U. Starke, K. Heinz, K. Müller, D. K. Saldin, P. de Andres and J. B. Pendry, *Surf. Sci.* 225, 242 (1990)
- 15 U. Starke, W. Oed, P. Bayer, F. Bothe, G. Fürst, P. L. de Andres, K. Heinz and J. B. Pendry, in *The Structure of Surfaces III*, eds S. Y. Tong, M. A. Van Hove, K. Takayanagi and X. D. Xie, Springer Verlag (Berlin, Heidelberg, New York), 1991
- 16 U. Starke, F. Bothe, W. Oed and K. Heinz, *Surf. Sci.* 232, 56 (1990)
- 17 W. Oed, U. Starke, F. Bothe and K. Heinz, *Surf. Sci.* 234, 72 (1990)
- 18 W. Oed, U. Starke, K. Heinz, K. Müller and J. B. Pendry, *Surf. Sci.* in press (1991), Proceedings of ECOSS, Salamanca, Spain (1990)
- 19 Z. P. Hu, B. C. Pan, W. C. Fan and A. Ignatiev, *Phys. Rev. B* 41, 9692 (1990)
- 20 A. W. Robinson, D. P. Woodruff, J. S. Somers, A. L. D. Kilcoyne, D. E. Ricken and A. M. Bradshaw, *Surf. Sci.* 237, 99 (1990)
- 21 M. J. Ashwin and D. P. Woodruff, *Surf. Sci.* 237, 108 (1990)
- 22 A. P. Baddorf and D. M. Zehner, *Surf. Sci.* 238, 255 (1990)
- 23 H. Niehus, R. Spitzl, K. Besocke and G. Comsa, *Phys. Rev. B* 43, 12619 (1991)
- 24 M. Bader, A. Puschmann, C. Ocal and J. Haase, *Phys. Rev. Lett.* 57, 3273 (1986)
- 25 R. Feidenhans'l, F. Grey, R. L. Johnson, S. G. J. Mochrie, J. Bohr and M. Nielsen, *Phys. Rev. B* 41, 5420 (1990)
- 26 S. R. Parkin, H. C. Zeng, M. Y. Zhou and K. A. R. Mitchell, *Phys. Rev. B* 41, 5432 (1990)
- 27 J. Wever, D. Wolf and W. Moritz, to be published (1991)
- 28 H. Dürr, Th. Fauster and R. Schneider, *Surf. Sci.* 244, 237 (1991)
- 29 G. Kleinle, J. Wintterlin, G. Ertl, R. J. Behm, F. Jona and W. Moritz, *Surf. Sci.* 225, 171 (1990)
- 30 R. Feidenhans'l, F. Grey, M. Nielsen, F. Besenbacher, F. Jensen, E. Laegsgaard, I. Steensgaard, K. W. Jacobsen, J. K. Norskov and R. L. Johnson, *Phys. Rev. Lett.* 65, 2027 (1990)
- 31 G. Kleinle, V. Penka, R. J. Behm, G. Ertl and W. Moritz, *Phys. Rev. Lett.* 58, 148 (1987)
- 32 D. T. VU Grimsby, Y. K. Wu and K. A. R. Mitchell, *Surf. Sci.* 232, 51 (1990)
- 33 M. A. Mendez, W. Oed, A. Fricke, L. Hammer, K. Heinz and K. Müller, *Surf. Sci.* submitted (1991)
- 34 Y. K. Wu and K. A. R. Mitchell, *Can. J. Chem.* 67, 1975 (1989)
- 35 W. Oed, B. Doetsch, L. Hammer, K. Heinz and K. Müller, *Surf. Sci.* 207, 55 (1988)
- 36 W. Nichtl, N. Bickel, L. Hammer, K. Heinz and K. Müller, *Surf. Sci.* 188, L729 (1987)
- 37 W. Nichtl, L. Hammer, K. Müller, N. Bickel, K. Heinz, K. Christmann and M. Ehsasi, *Surf. Sci.* 11, 201 (1988)
- 38 W. Oed, W. Puchta, N. Bickel, K. Heinz, W. Nichtl and K. Müller, *J. Phys. C* 21, 237 (1988)
- 39 K. Lehnberger, W. Nichtl-Pecher, W. Oed, K. Heinz and K. Müller, *Surf. Sci.* 217, 511 (1989)
- 40 M. Michl, W. Nichtl-Pecher, W. Oed, H. Landskron, K. Heinz and K. Müller, *Surf. Sci.* 220, 59 (1989)
- 41 W. Puchta, W. Nichtl, W. Oed, N. Bickel, K. Heinz and K. Müller, *Phys. Rev. B* 39, 1020 (1989)
- 42 H. Pfnür, G. Held, M. Lindroos and D. Menzel, *Surf. Sci.* 220, 43 (1989)
- 43 M. Lindroos, H. Pfnür, G. Held and D. Menzel, *Surf. Sci.* 222, 451 (1989)
- 44 Y. Joly, Y. Gauthier and R. Baudoing, *Phys. Rev. B* 40, 10119 (1989)

- 45 P. J. Rous, D. Jentz, D. G. Kelly, R. Q. Hwang, M. A. Van Hove and G. A. Somorjai, in *The Structure of Surfaces III*, eds S. Y. Tong, M. A. Van Hove, K. Takayanagi and X. D. Xie, Springer Verlag (Berlin, Heidelberg, New York), 1991, p.432
- 46 A. Wander, M. A. Van Hove and G. A. Somorjai, *Phys. Rev. Lett.*, in press
- 47 R. J. Hamers, Ph. Avouris and F. Bozso, *Journ. Vac. Sci. Techn. A*6, 508 (1988)
- 48 F. Shoji, K. Kashikara, K. Sumitomo and K. Oura, *Surf. Sci.* 242, 422 (1991)
- 49 B. I. Craig and P. V. Smith, *Surf. Sci.* 226, L55 (1990)
- 50 M. J. Bozack, M. J. Dresser, W. J. Choyke, P. A. Taylor and J. T. Yates, *Surf. Sci.* 184, L332 (1987)
- 51 G. Thornton, P. L. Wincott, R. McGrath, I. T. McGovern, F. M. Quinn, D. Norman and D. D. Vvedensky, *Surf. Sci.* 211/212, 959 (1989)
- 52 L. Incoccia, A. Balerna, S. Cramm, C. Kunz, F. Senf and I. Storzjohann, *Surf. Sci.* 189/190, 453 (1987)
- 53 P. V. Smith and A. Wander, *Surf. Sci.* 219, 77 (1989)
- 54 Y. Miyamoto and A. Oshiyama, *Phys. Rev. B* 41, 12680 (1990)
- 55 T. Urano, Y. Uchida, S. Hongo and T. Kanaji, *Surf. Sci.* 242, 39 (1991)
- 56 T. Kendelewicz, P. Soukiassian, R. S. List, J. C. Woicik, P. Pianetta, I. Lindau and W. E. Spicer, *Phys. Rev. B* 37, 7115 (1988)
- 57 Y. Ling, A. J. Freeman and B. Delley, *Phys. Rev. B* 39, 10144 (1989)
- 58 C. M. Wei, H. Huang, S. Y. Tong, G. S. Glander and M. B. Webb, *Phys. Rev. B* 42, 11284 (1990)
- 59 K. Kobayashi, S. Bluegel, H. Ishida and K. Terakura, *Surf. Sci.* 242, 349 (1991)
- 60 H. Huang, S. Y. Tong, W. S. Yang, H. D. Shih and F. Jona, *Phys. Rev. B* 42, 7483 (1990)
- 61 J. E. Northrup, *Phys. Rev. Lett.* 53, 683 (1984)
- 62 A. Kawazu and H. Sakama, *Phys. Rev. B* 37, 2704 (1988)
- 63 J. Nogami, S.-I. Park and C. F. Quate, *Surf. Sci.* 203, L631 (1988)
- 64 J. Zegenhagen, J. R. Patel, P. E. Freeland, D. M. Chen, J. A. Golovchenko, P. Bedrossian and J. E. Northrup, *Phys. Rev. B* 39, 1298 (1989)
- 65 K. M. Conway, J. E. McDonald, C. Norris, E. Vlieg and J. F. van der Veen, *Surf. Sci.* 215, 555 (1989)
- 66 H. Huang, C. M. Wei, H. Li, B. P. Tonner and S. Y. Tong, *Phys. Rev. Lett.* 62, 559 (1989)
- 67 R. L. Headrick, I. K. Robinson, E. Vlieg and L. C. Feldman, *Phys. Rev. Lett.* 63, 1253 (1989)
- 68 H. Huang, S. Y. Tong, J. Quinn and F. Jona, *Phys. Rev. B* 41, 3276 (1990)
- 69 T. Urano, M. Kaburagi, S. Hongo and T. Kanaji, *Appl Surf. Sci.* 41, 103 (1989)
- 70 J. R. Patel, J. A. Golovchenko, P. E. Freeland and H.-J. Gossmann, *Phys. Rev. B* 36, 7715 (1987)
- 71 R. L. Headrick and W. R. Graham, *Phys. Rev. B* 37, 1051 (1988)
- 72 M. Copel, R. M. Tromp and U. K. Koehler, *Phys. Rev. B* 37, 10756 (1988)
- 73 C. H. Patterson and R. P. Messmer, *Phys. Rev. B* 39, 1372 (1989)
- 74 J. R. Patel, P. E. Freeland, M. S. Hybertsen, D. C. Jacobsen and J. A. Golovchenko, *Phys. Rev. Lett.* 59, 2180 (1987)
- 75 J. E. Northrup, *Phys. Rev. B* 37, 8513 (1988)
- 76 T. Abukawa, C. Y. Park and S. Kono, *Surf. Sci.* 201, L513 (1988)
- 77 T. Takahashi, S. Nakatani, T. Ishikawa and S. Kikuta, *Surf. Sci.* 191, L825 (1987)